Research Paper

In Vivo Double Targeting of C26 Colon Carcinoma Cells and Microenvironmental Protumor Processes Using Liposomal Simvastatin

Lavinia Luput[1,2], Emilia Licarete[1,2], Denise Minerva Drotar[1], Andras-Laszlo Nagy[3], Alina Sesarman[1,2], Laura Patras[1,2], Valentin Florian Rauca[1,2], Alina Porfire[4✉], Dana Muntean[4], Marcela Achim[4], Ioan Tomuta[4], Laurian Vlase[4], Cornel Catoi[3], Nicolae Dragos[1,5], Manuela Banciu[1,2]

1. Department of Molecular Biology and Biotechnology, Faculty of Biology and Geology, Babes-Bolyai University, 400006, Cluj-Napoca, Romania;
2. Molecular Biology Centre, Institute for Interdisciplinary Research in Bio-Nano-Sciences, Babes-Bolyai University, 400271, Cluj-Napoca, Romania;
3. Department of Veterinary Toxicology, University of Agricultural Sciences and Veterinary Medicine, 400372, Cluj Napoca, Romania;
4. Department of Pharmaceutical Technology and Biopharmaceutics, Faculty of Pharmacy, University of Medicine and Pharmacy "Iuliu Hatieganu", 400012, Cluj-Napoca, Romania;
5. Taxonomy and Ecology Department, Institute of Biological Research, Cluj-Napoca, Romania.

✉ Corresponding author: Alina Porfire, Department of Pharmaceutical Technology and Biopharmaceutics, Faculty of Pharmacy, University of Medicine and Pharmacy "Iuliu Hatieganu" Cluj-Napoca, 41 Victor Babes, 400012 Cluj-Napoca, Romania. Tel/Fax: 0040264595770; Email: aporfire@umfcluj.ro

Abstract

Purpose: Besides cholesterol lowering effects, simvastatin (SIM) at very high doses possesses antitumor actions. Moreover our previous studies demonstrated that tumor-targeted delivery of SIM by using long-circulating liposomes (LCL) improved the therapeutic index of this drug in murine melanoma-bearing mice. To evaluate whether this finding can be exploited for future therapy of colorectal cancer the antitumor activity and the underlying mechanisms of long-circulating liposomal simvastatin (LCL-SIM) efficacy for inhibition of C26 murine colon carcinoma growth *in vivo* were investigated.

Materials and Methods: To find LCL-SIM dose with the highest therapeutic index, dose-response relationship and side effects of different LCL-SIM doses were assessed in C26 colon carcinoma-bearing mice. The underlying mechanisms of LCL-SIM versus free SIM treatments were investigated with regard to their actions on C26 cell proliferation and apoptosis (via tumor tissues immunostaining for PCNA and Bax markers), tumor inflammation (via western blot analysis of NF-κB production), angiogenesis (using an angiogenic protein array), and oxidative stress (by HPLC assessment of malondialdehyde).

Results: Our findings suggest that LCL-SIM antitumor activity on C26 colon carcinoma is a result of the tumor-targeting property of the liposome formulation, as free SIM treatment was ineffective. Moreover, LCL-SIM exerted significant antiproliferative and pro-apoptotic actions on C26 cells, notable suppressive effects on two main supportive processes for tumor development, inflammation and angiogenesis, and only slight anti-oxidant actions.

Conclusion: Our data proved that LCL-SIM antitumor activity in C26 colon carcinoma was based on cytotoxic effects on these cancer cells and suppressive actions on tumor angiogenesis and inflammation.

Key words: C26 colon carcinoma; long-circulating liposomal simvastatin; proliferation; apoptosis; inflammation; angiogenesis

Introduction

Chemotherapy for colorectal cancer (CRC) has many limitations such as development of chemoresistance and severe side effects [1], that require new approaches in terms of therapeutic agents and drug targeting. Thus, statins – the cholesterol-lowering agents could also be used as

anticancer drugs, due to their suppressive effects on the production of isoprenoids, the downstream products of mevalonate pathway – responsible for posttranslational modifications of a series of GTP-binding proteins (Ras, Rac, Rho), involved in cancer cell proliferation, inflammation, angiogenesis, invasion, and metastasis [2, 3]. Moreover, lipophilic statins are more efficient anticancer agents than hydrophilic statins mainly due to their capability of entering the cells via passive diffusion [4]. Among lipophilic statins, simvastatin (SIM) is one of the most used drug with known cytotoxic effects on various cancer models such as melanoma, head and neck, lung, ovarian, endometrial, and renal as well as CRC models [5-16]. Particularly in colon carcinoma models, several mechanisms were described for SIM administered alone or in combination with other antitumor agents, including inhibition of cancer cell proliferation, migration, and tumor angiogenesis [4, 11-15], as well as induction of apoptosis in carcinoma cells [13, 16]. Nevertheless these beneficial effects were described at very high concentrations of SIM (100 fold to 500 fold higher than those used for treatment of hypercholesterolemia) being accompanied by severe side effects [3]. Therefore, the main goal of our study was to investigate whether colon carcinoma-specific delivery of SIM by using long-circulating liposomes (LCL) might be an attractive solution for the necessity of high doses of this statin to achieve the antitumor activity while limiting side effects on healthy tissues. To our knowledge this colon carcinoma-targeting of SIM have never been described before. Notably, our preliminary data regarding the *in vitro* cytotoxicity of SIM incorporated in LCL on colon carcinoma cells have already suggested that liposomal encapsulation of SIM induced a higher intracellular drug concentration, and finally a stronger antitumor effect than free administration of SIM on these cells [4]. Moreover, previous studies demonstrated that incorporation of SIM in long-circulating liposomes offered the opportunity for this drug to inhibit almost totally the growth of B16.F10 murine melanoma *in vivo* whereas administration of SIM as unencapsulated form was ineffective in the same tumor model [5]. Passive tumor targeting of SIM was ensured by the long-circulation capacity of nanosized liposomes coated with polyethylene glycol (PEG). PEG-coated liposomes enabled their extravasation through the hyperpermeable vasculature of the tumors and accumulation in malignant tissue due to so called enhanced permeability and retention (EPR) effect [17]. To assess whether the antitumor activity of long-circulating liposomal SIM (LCL-SIM) could be exploited for future therapy of CRC, we investigated its anticancer potential in C26 murine colon carcinoma-bearing mice. Moreover the main mechanisms of the LCL-SIM antitumor activity in colon carcinoma *in vivo* were studied. Our results showed that LCL-SIM inhibited C26 colon carcinoma growth mainly via suppression of tumor angiogenesis and inflammation as well as through direct cytotoxic effects on C26 colon carcinoma cells.

Materials and methods

Preparation of LCL-SIM

LCL-SIM were prepared by using 1,2-dipalmitoyl-sn-glycero-3-phosphocholine (DPPC) (Lipoid GmbH, Germany), N-(carbonyl-methoxyp-olyethylenglycol-2000)-1,2-distearoyl-sn-glycero-3-ph osphoethanolamine (Na-salt) (MPEG-2000-DSPE) (Lipoid GmbH, Germany), cholesterol (CHO) (Sigma-Aldrich, Germany), and SIM (Biocon Limited, India) in a molar ratio of 9.5:0.5:1:2.2. Briefly, appropriate amounts of phospholipids (DPPC and MPEG-2000-DSPE in a molar ratio of 19:1), CHO and SIM were dissolved in ethanol in a round-bottomed flask, and the solvent was evaporated under reduced pressure at 40°C in a rotary evaporator, leading to the formation of a thin film on the surface of the flask. The remaining residual solvent was removed by maintaining the flask under nitrogen stream for 1 h. The film was subsequently hydrated with 5 ml phosphate buffered saline (PBS, pH = 7.8) for 15 min at 45°C. The liposomes were separated by centrifugation at 10000 x *g*, 15 min (Sigma 3-30K) and were diluted to 5 ml with the hydration buffer. Liposome size was reduced by multiple extrusions through polycarbonate membrane with final pore size of 0.1 µm using LiposoFast LF-50 equipment (Avestin Europe GmbH, Germany). Finally, LCL-SIM were stored at 4°C until analysis. The mean vesicles size and polydispersity of the liposomes were determined by dynamic light scattering method, using Zetasizer Nano ZS analyser (Malvern Instruments Co., Malvern, UK). Liposomal SIM concentration was determined using a HPLC/UV method in an Agilent 1100 chromatographic system (Agilent Technologies, Santa Clara, CA) coupled with an ultraviolet detector. The column used was Gemini C18 type (100 x 3mm, internal diameter 3µm) (Phenomenex, Torrance, CA) and the mobile phase consisted of a mixture of acetonitrile (72%) and water (28%). The separations were performed at room temperature and the detection was carried out at 238 nm. The liposomal SIM concentration was about 1300 µg/ml, corresponding to an encapsulation efficiency of 20%. Mean vesicles size of the liposomes was around 115 nm and the polydispersity values were lower than

0.15, both parameters showing a narrow size distribution and good potential for their passive accumulation in tumors [4, 5].

Cell line and *in vivo* murine tumor model

C26 murine colon carcinoma cells (Cell Lines Service GmbH, Eppelheim, Germany) were cultured in RPMI-1640 medium (Lonza, Group AG, Basel, Switzerland), supplemented with 10% heat-inactivated fetal bovine serum (HyClone; GE Healthcare Life Sciences, Logan, UT, USA), as monolayer at 37°C in a humidified atmosphere containing 5% CO_2. Colon carcinoma tumor model was generated by subcutaneous inoculation of 10^6 C26 cells in the right flank of 6-8 weeks-old male Balb/c mice (Cantacuzino Institute, Bucharest, Romania). Body weight of mice was monitored daily during treatments. Mice were kept on a 12:12 light-dark cycle with standard rodent chow and water available *ad libitum*. The tumor became palpable at day 7 after cell inoculation. Tumor size was measured daily and tumor volume was determined according to the formula: $V = 0.52a^2b$, where *a* is the smallest and *b* is the largest superficial diameter. Experiments were performed according to the national regulations and were approved by university animal experiments ethical committee (registration no.31375/06.04.2015).

Dose-response assessment

To assess the optimal dose of SIM encapsulated in LCL with the highest therapeutic index on C26 colon carcinoma, mice were injected *i.v.* (in caudal vein), twice at days 8 and 11 after tumor cell inoculation with the following doses of LCL-SIM: 2.5, 5, 7.5, and 10 mg/kg. Tumor size was measured daily and mice were sacrificed at day 16 after tumor induction, when first tumors from the control group reached the volume of 2000 mm^3 that represents the safe volume to prevent C26 carcinoma metastasis [18].

Assessment of the adverse effects of treatments tested

As incorporation of SIM in LCL offered the opportunity to achieve antitumor activities at much lower doses of this drug compared to its free administration [13] the adverse effects associated with the administration of low-dose statin therapies [19, 20] as well as of long-circulating liposomal formulations [21] were assessed. Thus, adverse effects of different treatments were investigated by monitoring body weight loss and weight loss of certain organs (spleen, liver, and kidney) [19-21]. The body weight was measured every day and the organs were weighed after mice sacrification.

Effects of LCL-SIM *versus* free SIM on tumor growth

LCL-SIM and free SIM (administered as unencapsulated SIM solubilized in 10% dimethylsulfoxide (DMSO)) were administered in caudal vein at a dose of 5 mg/kg at days 8 and 11 after tumor cell inoculation. As controls were used tumor-bearing mice treated with PBS, empty LCL (*i.e.* devoid of drug) and 10% DMSO. Each experimental group were composed by five animals. Tumor volume was measured daily and calculated as described above. On day 12, mice were sacrificed and tumors were measured and collected.

Immunohistochemical examination of tumor tissue for cytotoxicity of treatments

For the immunohistochemical analysis, the sections were dewaxed and rehydrated. Heat-mediated epitope retrieval was performed by samples immersion in boiling citrate buffer pH 6, using a pressure-cooker. Sections were cooled in citrate buffer at room temperature and washed in triphosphate-buffered saline (TBS). Endogenous peroxidase activity was blocked using 3% hydrogen peroxide in methanol for 10 minutes. Sections were incubated overnight with the primary antibodies: monoclonal mouse anti-rat proliferating cell nuclear antigen (PCNA, Clone PC 10, dilution 1:300, DakoCytomation, Glostrup, Denmark) and polyclonal rabbit anti-mouse Bax (Bcl-2-associated X protein, bcl-2-like protein 4, ab7977, dilution 1:75, Abcam, Newcastle, UK). For detection Novolink Max-Polymer detection system (Novocastra, Newcastle, UK) was used. Positive reaction was visualized using 3,3'-diaminobenzidine (DAB). Afterwards, sections were counterstained with Gill 2 haematoxylin, dehydrated and mounted. Then the slides were examined under a microscope Olympus BX 51. The images were taken with Olympus UC 30 digital camera and processed by using image acquisition and processing program Olympus Stream Basic. The numbers of PCNA- and Bax- positive cells were assessed by counting 1000-1500 nuclei on several non-overlapping fields for each slide. The data were expressed as mitotic and apoptotic index represented by percentage of PCNA-positive cells (brown stained nuclei) [22], respectively percentage of Bax-positive cells (brown stained cytoplasm) from the total number of counted cells [23]. The positive cells for PCNA or Bax protein were expressed by using quantity score that represent the percentage of the number of immunoreactive cells from the total number of cells analyzed. As negative cells for either PCNA or Bax were cells that did not present the specific staining for each marker analyzed.

Preparation of tumor tissue lysates

After mice were sacrificed, tumors were isolated, weighed and pooled tumor tissue lysates for each group and instant frozen in liquid nitrogen. Tumor tissues were incubated with lysis buffer (PBS with 1% Triton X, with protease and phosphatase inhibitors cocktail tablets from Roche Diagnostics GmbH, Mannheim, Germany) for 30 min on ice and lysed using a Potter-tissue homogenizer (Thomas Scientific, Swedesboro, New Jersey, USA), centrifuged at 15 000 x g for 10 min at 4˚C, and the supernatant was collected. The protein concentration of the supernatant was measured using biuret method [24]. Tumor tissue lysates were used for further molecular measurements.

Assessment of NF-κB intratumor production by western blot analysis

The effect of the treatments tested on the intratumor expression level of NF-κB – a key inflammatory transcription factor for maintaining the C26 colon carcinoma phenotype [25], was assessed by western blot analysis. The production of the active form of NF-κB (when p65 subunit of NF-κB is phosphorylated, pNF-κB-p65) and the total NF-κB-p65 subunit (pNF-κB-p65 and inactive form of NF-κB when p65 subunit is unphosphorylated) from tumor tissue lysates was determined. Two micrograms of total protein was loaded per lane onto a 10% polyacrylamide gel. Electrophoresis and electro-transferred onto a nitrocellulose membrane were performed as previously described [25]. Specific primary antibodies, polyclonal rabbit IgG anti-mouse pNF-κB p65 (diluted 1:500 in TBS-T, with 5% skimmed milk powder) and monoclonal mouse IgG anti-mouse NF-κB p65 (diluted 1:500 in TBS-T, with 5% skimmed milk powder) (Santa Cruz Biotechnology, Dallas, Texas, USA), and secondary antibodies: goat IgG anti-mouse IgG HRP-conjugated (diluted 1:4000 TBS-T, with 5% skimmed milk powder) or goat IgG anti-rabbit IgG HRP-conjugated (diluted 1:4000 TBS-T, with 5% skimmed milk powder) (Santa Cruz Biotechnology, Dallas, Texas, USA) were used. The antibodies for determination of β-actin as loading control were rabbit polyclonal IgG anti-mouse β-actin (diluted 1:1000 TBS-T, with 5% skimmed milk powder) and polyclonal IgG anti-rabbit IgG HRP-conjugated (diluted 1:4000 TBS-T, with 5% skimmed milk powder) (Santa Cruz, Dallas, Texas, USA). The detection was performed by using Clarity™ Western ECL kit (Bio-Rad Laboratories, Hercules, CA, USA) and the membranes were exposed to an X-ray film (Kodak, Knoxville, TN, USA) for 2 min. The films were developed and analysed using TotalLab Quant Software version 12 for Windows. The expression levels of the active form pNF-κB-p65 was determined and represented as percentage from the total amount of NF-κB-p65 subunit. The final results represent mean±SD of two independent experiments.

Testing the angiogenic protein production in tumors by protein array

The expression levels of angiogenic proteins in tumor tissue were investigated by performing a screening for 24 proteins involved in angiogenesis using RayBio® Mouse Angiogenic Cytokine Antibody Array kit (RayBiotech Inc., Norcross, GA, USA) as described previously [26]. The protein expression levels were quantified by measuring the intensity of the colour of each spot on the membranes, in comparison to the positive control spots already bound to the membranes, using TotalLab Quant Software version 12 for Windows. The expression of each angiogenic protein in tumor tissue lysates was determined in duplicate. The final results represent mean ± SD of two independent experiments.

Assessment of malondialdehyde levels in tumors by HPLC analysis

To evaluate the influence of different treatments on tumor oxidative stress the amount of malondialdehyde (MDA) from tumor tissue lysates was quantified through high-performance liquid chromatography (HPLC) as previously described [25]. Data were expressed as μM MDA and were normalized to the protein concentration in tumor tissue lysates. Each sample was determined in triplicate.

Statistical analysis

Data from different experiments were reported as mean ± SD. Statistical comparisons of the overall effects of different treatments on tumors were evaluated by one-way ANOVA with Dunnett's post-test for multiple comparisons. The tumor volume doubling time (DT) was estimated by using an exponential tumor growth equation. The differences between the effects of different treatments on angiogenic proteins production were analysed by two-way ANOVA with Bonferroni correction for multiple comparisons using GraphPad Prism version 6 for Windows, GraphPad Software (San Diego, CA). A value of $p < 0.05$ was considered significant.

Results

Antitumor activity of LCL-SIM: dose-response relationship

To evaluate the relationship between different doses of LCL-SIM and their antitumor activity, mice

received two *i.v.* injections of indicated doses, on day 8 and 11 after tumor induction. The tumor volumes were measured until day 16 when first tumors from the control group reached the maximum volume of 2000 mm³. The results were shown as tumor volumes at day 16 in Fig.1A and areas under the tumor growth curves (AUTC) in Fig.1 B. For all doses tested the values of tumor volumes as well as AUTC were much smaller than those obtained in control group and a significant negative correlation between dose and response was noted (Spearman correlation coefficient of -1, *p*=0.01). Notably, the maximal antitumor activity was already achieved at a dose of 5 mg/kg of SIM. Thus, at this dose, tumor volumes were reduced with more than 70% (Fig.1A) and the deceleration of tumor growth at day 16 after tumor induction was about 62% (Fig. 1B) compared with the growth of tumors from the control group.

Adverse effects

Apparently no changes in weight of certain organs were noted for any treatment tested. Only the highest doses of 7.5 and 10 mg/kg of LCL-SIM showed a significant body weight loss of 23% compared to the initial weight of animals. Therefore, the lowest dose of LCL-SIM (5 mg/kg) that exerted strong inhibitory action on tumor growth without occurrence of visible adverse effects was chosen to be tested throughout the experiments conducted for testing the mechanisms of the antitumor activity of this liposomal statin formulation.

Effect of LCL-SIM *versus* free SIM on tumor growth

To compare the effects of 5 mg/kg LCL-SIM and the same dose of free SIM on C26 colon carcinoma-bearing mice, treatments were administered at day 8 and day 11 after tumor cell inoculation. The antitumor activities were evaluated by measuring the tumor volumes at day 12 (the day when mice were sacrificed) (Fig. 2A) and AUTC (Fig. 2B) and the tumor volume doubling time (DT) until day 12. No growth differences were noted among the control groups (tumors from mice treated with PBS, empty liposomes or 10% DMSO) (*p*>0.05) (data not shown). Notably, tumor volumes from LCL-SIM-treated group were 50% smaller as compared with those noted from controls (*p*<0.01, Fig.2A) while free administration of SIM did not affect this tumor growth parameter (Fig.2A). In line with tumor volume data, AUTC were significantly reduced after LCL-SIM treatment as compared to free drug-treated tumors or controls (*p*<0.05, Fig. 2B). Moreover DT of tumors confirmed the inhibitory action of LCL-SIM on tumor growth since DT for C26

tumors that received the liposomal formulation was about 2 times longer than DT of tumors from free SIM –treated group or control groups (DT of LCL-SIM-treated tumors was about 4.1 days, and DT for SIM-treated tumor or control tumors was about 2.2 days). Altogether these data suggested that the antitumor activity of LCL-SIM was enabled by tumor-targeting capacity of the liposomes that augmented intratumor statin accumulation and thereby amplified the inhibitory effects of SIM on C26 colon carcinoma.
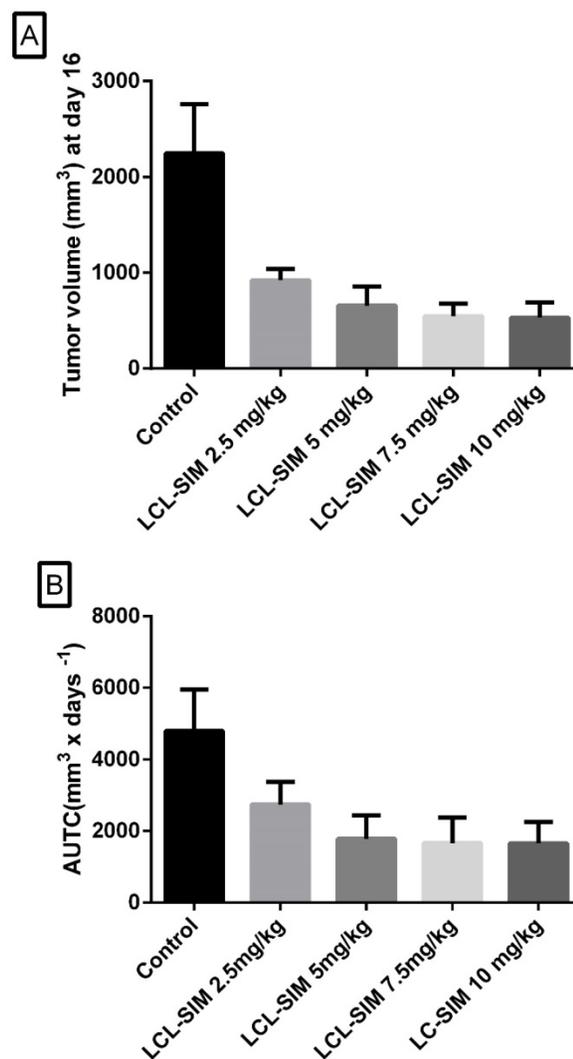

Figure 1. Antitumor activity of different doses of LCL-SIM. Mice received two *i.v.* injections of either formulation at day 8 and day 11, after tumor cell inoculation. The data were reported at day 16 after cell inoculation (the day when first tumors from the control group reached the maximum volume of 2000 mm³). **A. Tumor volumes at day 16. B. Areas under the tumor growth curves (AUTC) until the day 16 after tumor induction.** The results were expressed as mean ± SD of five mice; Control - untreated group (group treated with PBS); 2.5 mg/kg LCL-SIM - group treated with 2.5 mg/kg LCL-SIM at days 8 and 11 after tumor cell inoculation; 5 mg/kg LCL-SIM - group treated with 5 mg/kg LCL-SIM at days 8 and 11 after tumor cell inoculation; 7.5 mg/kg LCL-SIM - group treated with 7.5 mg/kg LCL-SIM at days 8 and 11 after tumor cell inoculation; 10 mg/kg LCL-SIM - group treated with 10 mg/kg LCL-SIM at days 8 and 11 after tumor cell inoculation.
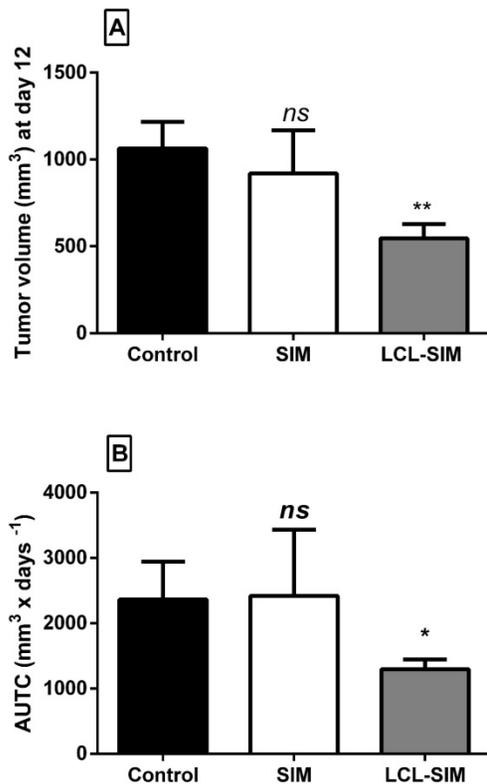
Figure 2. Antitumor activities of LCL-SIM and free SIM in C26 colon carcinoma-bearing mice. Mice received two *i.v.* injections of either formulation at day 8 and day 11, after cell inoculation. The data were reported at day 12 after tumor cell inoculation (the day when mice were sacrificed) **A. Tumor volumes at day 12 in different treatment groups. B. Areas under the tumor growth curves (AUTC) until day 12.** The results were expressed as mean ± SD of five mice; Control - untreated group (group treated with PBS); SIM - group treated with 5 mg/kg free SIM at days 8 and 11 after tumor cell inoculation; LCL-SIM - group treated with 5 mg/kg LCL-SIM at days 8 and 11 after tumor cell inoculation. To compare the effects of each treatment on tumors *in vivo* with controls (tumors in mice treated with PBS), one-way ANOVA with Dunnett's Test for multiple comparisons was used and the *p* values are indicated as follows: *ns*, not significant (*p*>0.05); *, *p*<0.05; **, *p*<0.01.

Cytotoxic effects of LCL-SIM on tumor tissue

To link the antitumor activity of LCL-SIM with its direct cytotoxic effects on C26 colon carcinoma cells, the proliferation as well as apoptosis-related molecules were assessed by immunohistochemical analysis of tumors after different treatments and the results were shown in Fig. 3 A-F. Thus, tumors were evaluated immunohistochemically for the expression of proliferating cell nuclear antigen (PCNA) (Fig. 3 A-C) as well as of Bax apoptotic protein (Fig. 3D-F). Our data suggested that the antitumor activities of different treatments correlated negatively with mitotic index (Spearman correlation coefficient =-0.82, *p*=0.0001) and positively with apoptotic index (Spearman correlation coefficient = 0.82, *p*=0.0014). More precisely, LCL-SIM-treated tumors presented much lower proliferative potential by 50-60% compared to either control tumors or SIM-treated tumors (Fig. 3A-C and Table 1). After LCL-SIM administration, the intratumor expression of the

apoptotic protein Bax increased slightly by 15% compared to its production in SIM-treated tumors and moderately by 36% compared to the same protein expression in control tumors (Fig. 3D-F and Table 1).

Table 1. Quantification of immunoreactive cells for PCNA and Bax proteins after different treatments

	Quantity score		
	Control	SIM	LCL-SIM
PCNA-positive cells	+++	++	+
Bax-positive cells	++	++	+++

The amount of immunoreactive cells for each specific protein were scored as follows: **+** represented less than 20% of PCNA - or Bax- positive cells from total number of cells analyzed); **++** represented 21-35% of PCNA - or Bax- positive cells from total number of cells analyzed); **+++** represented higher than 36% of PCNA- or Bax- positive cells from total number of cells analyzed).

Effect of LCL-SIM treatment on the C26 colon carcinoma production of NF-κB

To investigate whether the antitumor activity of LCL-SIM was exerted through the modulation of the production of the key inflammatory transcription factor, NF-κB [25], the levels of the active form of this protein (NF-κB with p65 subunit phosphorylated, pNF-κB-p65) as well as the production of total NF-κB in C26 colon carcinoma were assessed via western blot analysis and shown in Fig.4A. The results were presented as percentages of pNF-κB-p65 production from the amount of total NF-κB-p65 subunit in tumor tissues (Fig. 4B). Although, the intratumor levels of total NF-κB were similar in all experimental groups, the administration of LCL-SIM reduced significantly the levels of the active form of NF-κB by 51% (*p*<0.05) compared to its production in control tumors whereas the SIM administered as free form did not affect the C26 tumor production of pNF-κB-p65 (Fig. 4A and B).

Effects of LCL-SIM on tumor angiogenesis

To link the antitumor activity of LCL-SIM in C26 colon carcinoma with its effects on tumor angiogenesis we investigated the effects of liposomal administration of SIM and free SIM on the production of 24 proteins involved in angiogenesis and inflammation from tumor tissue, using RayBio Mouse Angiogenic Cytokine Antibody Array. The effects of LCL-SIM and free SIM on the C26 tumor production of the pro-angiogenic proteins were presented in detail in Table 2. The levels of most of the pro-angiogenic proteins were reduced significantly in case of liposomal and free SIM administration compared to their control levels. Nevertheless, the overall reduction of pro-angiogenic proteins was stronger and statistically significant after LCL-SIM treatment compared with that induced by free SIM administration. On average, the effect of LCL-SIM on pro-angiogenic protein levels was 22% higher than the

effect of free SIM on the same protein production ($p<0.0001$). More specifically, LCL-SIM treatment inhibited by 30-60% the expression of interleukin 9 (IL-9), basic fibroblast growth factor (bFGF), and leptin and by 60-90% the production of granulocyte colony-stimulating factor (G-CSF), granulocyte-macrophages colony-stimulating factor (GM-CSF), interleukin 1β (IL-1β), interleukin 6 (IL-6), tumor necrosis factor α (TNF-α), eotaxin, Fas ligand (FasL), and vascular endothelial growth factor (VEGF). Only the production of monocyte chemoattractant protein-1 (MCP-1) was stimulated strongly (by 75%) after LCL-SIM administration while free SIM treatment stimulated by 55-85% the levels of bFGF, interleukin 12 subunit p40 (IL-12p40), thrombopoietin (TPO), and also MCP-1. In the case of anti-angiogenic proteins, both treatments exerted similar strong stimulatory effects on the levels of tissue inhibitor of metalloproteinases-1 (TIMP-1) and platelet factor-4 (PF-4) (75-165% stimulation compared to control levels of these proteins) and moderate reducing effects on the levels of tissue inhibitor of metalloproteinases-2 (TIMP-2) (45-65% reduction compared to control protein production) (Table 3). Moreover, SIM administration stimulated the production of interleukin 12 subunit p70 (IL-12p70) (by 104%) and monokine induced by interferon-γ (MIG) (by 55%) while LCL-SIM exerted notable reducing effects (by 50%) on the intratumor production of interferon-γ (IFN-γ) and MIG (Table 3).

Table 2. Effects of LCL-SIM and free SIM on pro-angiogenic protein production on C26 tumor tissues.

Pro-angiogenic proteins	Percentage of inhibition (-) and stimulation (+) of pro-angiogenic proteins levels in the C26 colon carcinoma after different treatments compared to their control levels	
	SIM	LCL-SIM
G-CSF	-52.89 ± 0 (****)	-83.11 ± 2.85 (****)
GM-CSF	-71.22 ± 0 (****)	-69.66 ± 6.82 (****)
M-CSF	27.57 ± 3.84 (ns)	20.77 ± 6.84 (ns)
IGF-II	9.32 ± 0.15 (ns)	-6.13 ± 5.71 (ns)
IL-1α	1.13 ± 17.06 (ns)	-22.08 ± 0.14 (ns)
IL-1ß	-79.20 ± 9.78 (****)	-76.02 ± 1.36 (****)
IL-6	-66.88 ± 15.64 (****)	-91.25 ± 0.74 (****)
IL-9	-32.48 ± 4.33 (*)	-32.1 ± 10.56 (*)
IL-12p40	57.37 ± 34.13 (****)	3.34 ± 6.29 (ns)
IL-13	-29.18 ± 10.33 (*)	-26.8 ± 2.68 (ns)
TNF-α	-72.38 ± 1.94 (****)	-70.96 ± 3.9 (****)
MCP-1	85.36 ± 15.36 (****)	73.66 ± 9.5 (****)
Eotaxin	-86.46 ± 0 (****)	-88.94 ± 5.67 (****)
FasL	-11.8 ± 7.52 (ns)	-60.38 ± 23.6 (****)
bFGF	55.32 ± 24.32 (****)	-59.77 ± 18.41 (****)
VEGF	-66.08 ± 0.17 (****)	-71.34 ± 1.46 (****)
Leptin	-42.69 ± 13.14 (***)	-48.25 ± 9.8 (***)
TPOa	86.08 ± 0.46 (****)	23.96 ± 4.5 (ns)

The protein levels in tumors after different treatments were compared to protein levels in control tumors. The results represented the mean ± SD of two independent measurements. *ns*, not significant, $p>0.05$; *, $p<0.05$; **, $p<0.01$.***; $p<0.001$; ****, $p<0.0001$. ᵃTPO, thrombopoietin.

Table 3. Effects of LCL-SIM and free SIM on anti-angiogenic protein production on C26 tumor tissues.

Anti-angiogenic proteins	Percentage of inhibition (-) and stimulation (+) of anti-angiogenic proteins levels in the C26 colon carcinoma after different treatments compared to their control levels	
	SIM	LCL-SIM
TIMP-1	75.52 ± 14.27 (****)	99.89 ± 1.2 (****)
TIMP-2	-44.11 ± 3.05 (***)	-64.33 ± 3.99 (****)
PF-4	162.56 ± 39.74 (****)	120.91 ± 11.48 (****)
IL-12p70	103.64 ± 24.41 (****)	25.03 ± 3.37 (ns)
IFN-γ	-8.48 ± 5.57 (ns)	-50.37 ± 0.16 (****)
MIG	54.74 ± 8.52 (****)	-49.78 ± 4.21 (****)

The protein levels in tumors after different treatments were compared to protein levels in control tumors. The results represented the mean ± SD of two independent measurements; *ns*, not significant, $p>0.05$; ***; $p<0.001$; ****, $p<0.0001$.

Effect of LCL-SIM treatment on tumor oxidative stress

To evaluate the involvement of oxidative stress in the antitumor activity of LCL-SIM, we measured the intratumor levels of MDA – a by-product of lipid peroxidation [27] and thus a marker for oxidative stress and the results were shown in Fig. 5. Our data suggested that LCL-SIM as well as free SIM treatment exerted only slight anti-oxidant actions on tumor microenvironment as intratumor levels of MDA after each treatment were reduced by 10-16% compared with MDA levels in control tumors.

Discussion

The present study is a follow-up of our earlier data regarding the antitumor activity of LCL-SIM on B16.F10 melanoma *in vivo* [5]. To evaluate whether this finding can be exploited for future therapy of CRC the antitumor activity of LCL-SIM in C26 colon carcinoma-bearing mice was investigated which to our knowledge has never been tested before. Thus, the dose of SIM encapsulated in LCL (5 mg/kg) with the highest therapeutic index in C26 colon carcinoma *in vivo* was selected (Fig. 1A and B). In accordance with our previous observations [5] the antitumor efficacy of LCL-SIM in murine carcinoma was tightly linked to tumor-targeting capacity of LCL since the administration of the same dose of free SIM did not exert any antitumor activity (Fig. 2A and B). Thus, LCL-SIM could accumulate passively into the malignant tissue due to the EPR effect as well as its physico-chemical properties (including size and PEG coating of liposomal particles) [5, 17], intensifying the anticancer effects of SIM. Furthermore, to gain more insight into the *in vivo* mechanisms of LCL-SIM responsible for C26 carcinoma growth inhibition we investigated the cytotoxicity with regard to the cancer cell proliferation and apoptosis as well as the modulatory actions of this liposomal formulation on the supportive processes for tumor development,

such as tumor inflammation, angiogenesis, and oxidative stress. The cytotoxic effects of LCL-SIM on C26 tumors were assessed by the immuno-histochemical analysis of the related molecules, PCNA – a marker for proliferation [22] and Bax – a marker for apoptosis [23]. Our results showed that LCL-SIM exerted significant antiproliferative (Fig. 3 A-C, Table 1) and pro-apoptotic actions (Fig. 3D-F, Table 1) on colon carcinoma that correlated strongly with the antitumor efficacy of this liposomal formulation. Our findings are also supported by previous studies regarding SIM induction of apoptosis in human myeloid KBM-5 cells through the inhibition of NF-κB activation [28]. It is known that inhibition of this transcription factor represents a potent therapeutic strategy in CRC since the intratumor activation and constitutive expression of NF-κB was correlated with tumor growth and progression [25, 29]. In line with these studies, our data showed that the intratumor levels of activated NF-κB were reduced strongly in LCL-SIM-treated group compared with the control protein production (Fig. 4A and B). Therefore, the suppression of the NF-κB activation in colon carcinoma might be one of the major causes for the antitumor activity of LCL-SIM in the tumor model tested. Moreover, the levels of several pro-angiogenic proteins, IL-1β, IL-6, and TNF-α, which constitutively activate NF-κB and finally enhance the angiogenic and metastatic capacity of tumor cells [25, 29] were strongly reduced after LCL-SIM treatment (Table 2). Since NF-κB controls the expression of several genes encoding for proteins involved in tumor angiogenesis and inflammation [25, 30] LCL-SIM-mediated suppression of NF-κB activation might also be an explanation for the anti-inflammatory and anti-angiogenic actions of

this liposomal statin on C26 tumors (Tables 2 and 3). Thus, the intratumor levels of 11 out of 18 pro-angiogenic proteins tested were moderately to strongly reduced after LCL-SIM treatment (Table 2). Interestingly, the C26 tumor production of the pro-inflammatory chemokine, MCP-1 was stimulated substantially after LCL-SIM treatment as well as free administration of SIM. Although, this finding could show a limitation of the antitumor efficacy of the LCL-SIM, recent studies associated the high level of MCP-1 with the M1 polarization of macrophages [31]. Thus, the increased production of MCP-1 could favour the antitumor phenotype of macrophages emphasizing the inhibitory effects of LCL-SIM on tumor angiogenesis. Nevertheless further investigations are needed to prove the "re-education" of tumor-associated macrophages to antitumor, "M1-like" macrophages as a result of LCL-SIM administration in C26 colon carcinoma. It is worth to mention that LCL-SIM stimulated significantly the production of two anti-angiogenic proteins (TIMP-1 and PF-4) (Table 3), that could enhance anti-angiogenic effect of this treatment. Although the anti-angiogenic actions on tumor microenvironment were also exerted by SIM administration as free drug, the amplitude of these effects were lower than those determined by LCL-SIM (Tables 2 and 3). Furthermore, SIM administered as unencapsulated drug did not affect NF-κB activation (Fig.4A and B). Altogether our data demonstrated that the antitumor efficacy of LCL-SIM in C26 colon carcinoma *in vivo* was also based on both anti-angiogenic and anti-inflammatory effects of this liposomal statin on tumors.
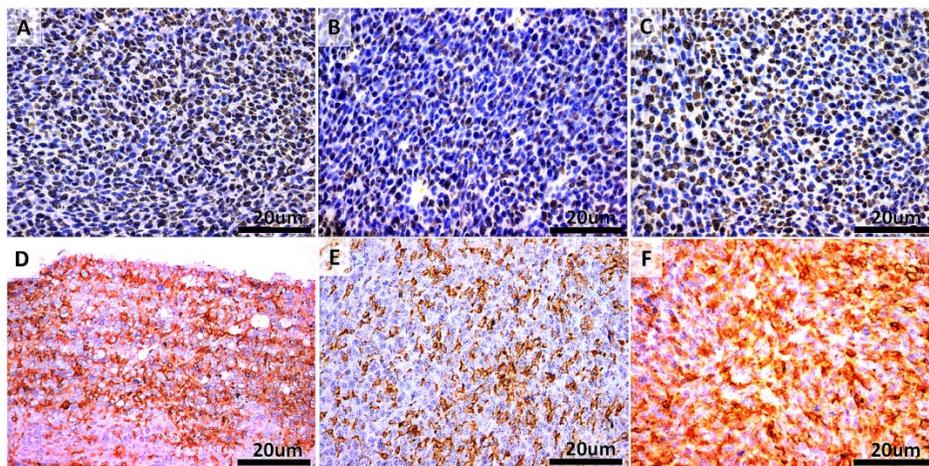

Figure 3. Immunohistochemical analysis of the cytotoxic effects of different treatments on C26 murine colon carcinoma *in vivo*. A-C. PCNA expression in tumors. Cells that present nuclear staining in brown are PCNA-positive cells. Sections were counterstained with Gill 2 hematoxylin. **D-F. Bax expression in tumors.** Cells that present cytoplasmic staining in brown are Bax-positive cells. Sections were counterstained with Gill 2 hematoxylin. **A** and **D-**Control (untreated group); **B** and **E-** group treated with 5 mg/kg SIM at days 8 and 11 after tumor cell inoculation; **C** and **F-** group treated with 5 mg/kg LCL-SIM at days 8 and 11 after tumor cell inoculation. Scale bars of 20 μm and original magnification of 400*X*.
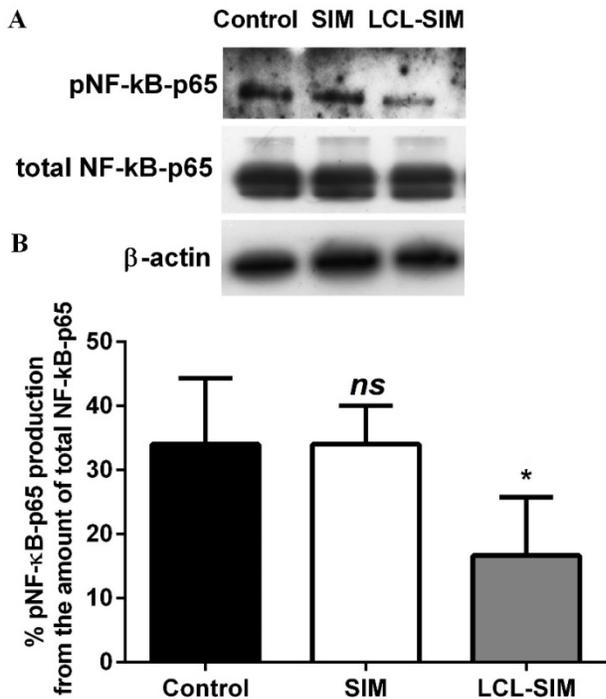
Figure 4. Effect of LCL-SIM on the expression of NF-κB in tumors analysed by Western blot. A. The levels of the active form of NF-κB (when the p65 subunit of NF-κB is phosphorylated, pNF-κB-p65), total NF-κB (total amount of the subunit p65 of NF-κB, in active as well as inactive form, total NF-κB-p65) and β-actin in tumors. Control - untreated group; SIM - group treated with 5 mg/kg free SIM at days 8 and 11 after tumor cell inoculation; LCL-SIM - group treated with 5 mg/kg LCL-SIM at days 8 and 11 after tumor cell inoculation. β-actin was used as loading control. **B.** Percentages of the amount of the active form of NF-κB over the total NF-κB amount. The results were expressed as mean ± SD of four independent measurements. To compare the effects of each treatment on the tumor levels of the proteins tested *in vivo* with their control levels, one-way ANOVA with Dunnett's Test for multiple comparisons was used and the *p* values are indicated as follows: *ns*, not significant ($p > 0.05$); *, $p < 0.05$.
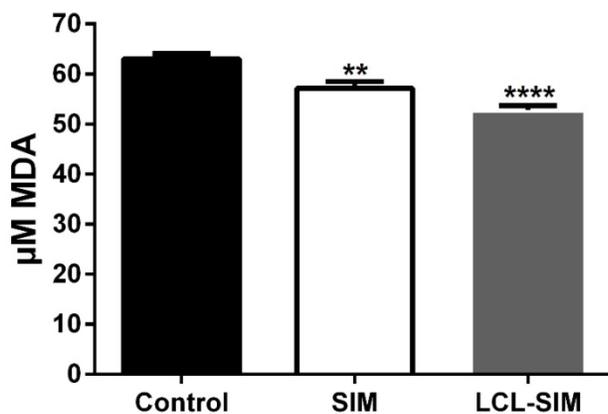

Figure 5. The effect of LCL-SIM treatment on the MDA levels in C26 colon carcinoma. The results are expressed as mean ± SD of three independent measurements and compared with control tumors levels of MDA; Control - untreated group (group treated with PBS); SIM - group treated with 5 mg/kg free SIM at days 8 and 11 after tumor cell inoculation; LCL-SIM 5 mg/kg - group treated with 5 mg/kg LCL-SIM at days 8 and 11 after tumor cell inoculation; To compare the effects of each treatment on the tumor levels of the MDA with its control levels, one-way ANOVA with Dunnett's Test for multiple comparisons was used and the *P* values are indicated as follows:** ($p < 0.01$), **** ($p < 0.0001$).

Since previous studies demonstrated the involvement of tumor oxidative targeting in the antitumor activity of LCL-SIM in B16.F10 melanoma-bearing mice [5], we quantified an important oxidative stress marker in tumor tissue lysates, MDA (Fig.5). Our results suggested that that the antitumor activity of LCL-SIM did not involve the inhibition of tumor oxidative stress, as the levels of MDA were only slightly affected by LCL-SIM administration in colon carcinoma-bearing mice.

Taken together, our data proved that the incorporation of SIM in LCL offers an increased antitumor activity in C26 murine colon carcinoma-bearing mice. One of the future issues is to further identify the potential of this treatment to "re-educate" tumor-associated macrophages to fight against cancer.

Abbreviations

CRC: colorectal cancer; SIM: simvastatin; LCL-SIM: long-circulating liposomal simvastatin; TPO: thrombopoietin; MDA: malondialdehyde; AUTC: areas under the tumor growth curves.

Acknowledgements

Competing Interests

The authors have declared that no competing interest exists.

References

1. Longley DB, Johnston PG. Molecular mechanisms of drug resistance. The Journal of pathology. 2005; 205: 275-92.
2. Chan KK, Oza AM, Siu LL. The statins as anticancer agents. Clinical cancer research: an official journal of the American Association for Cancer Research. 2003; 9: 10-9.
3. Licarete E, Sesarman A, Banciu M. Exploitation of pleiotropic actions of statins by using tumour-targeted delivery systems. Journal of microencapsulation. 2015; 32: 619-31.
4. Porfire A, Tomuta I, Muntean D, Luca L, Licarete E, Alupei MC, et al. Optimizing long-circulating liposomes for delivery of simvastatin to C26 colon carcinoma cells. Journal of liposome research. 2015; 25: 261-9.
5. Alupei MC, Licarete E, Patras L, Banciu M. Liposomal simvastatin inhibits tumor growth via targeting tumor-associated macrophages-mediated oxidative stress. Cancer letters. 2015; 356: 946-52.
6. Takeda I, Maruya S, Shirasaki T, Mizukami H, Takahata T, Myers JN, et al. Simvastatin inactivates beta1-integrin and extracellular signal-related kinase signaling and inhibits cell proliferation in head and neck squamous cell carcinoma cells. Cancer science. 2007; 98: 890-9.
7. Khanzada UK, Pardo OE, Meier C, Downward J, Seckl MJ, Arcaro A. Potent inhibition of small-cell lung cancer cell growth by simvastatin reveals selective

functions of Ras isoforms in growth factor signalling. Oncogene. 2006; 25: 877-87.

8. Stine JE, Guo H, Sheng X, Han X, Schointuch MN, Gilliam TP, et al. The HMG-CoA reductase inhibitor, simvastatin, exhibits anti-metastatic and anti-tumorigenic effects in ovarian cancer. Oncotarget. 2016; 7: 946-60.

9. Schointuch MN, Gilliam TP, Stine JE, Han X, Zhou C, Gehrig PA, et al. Simvastatin, an HMG-CoA reductase inhibitor, exhibits anti-metastatic and anti-tumorigenic effects in endometrial cancer. Gynecologic oncology. 2014; 134: 346-55.

10. Fang Z, Tang Y, Fang J, Zhou Z, Xing Z, Guo Z, et al. Simvastatin inhibits renal cancer cell growth and metastasis via AKT/mTOR, ERK and JAK2/STAT3 pathway. PloS one. 2013; 8: e62823.

11. Bergman M, Salman H, Djaldetti M, Bessler H. Statins as modulators of colon cancer cells induced cytokine secretion by human PBMC. Vascular pharmacology. 2011; 54: 88-92.

12. Park HJ, Kong D, Iruela-Arispe L, Begley U, Tang D, Galper JB. 3-hydroxy-3-methylglutaryl coenzyme A reductase inhibitors interfere with angiogenesis by inhibiting the geranylgeranylation of RhoA. Circulation research. 2002; 91: 143-50.

13. Cho SJ, Kim JS, Kim JM, Lee JY, Jung HC, Song IS. Simvastatin induces apoptosis in human colon cancer cells and in tumor xenografts, and attenuates colitis-associated colon cancer in mice. International journal of cancer. 2008; 123: 951-7.

14. Lee SJ, Lee I, Lee J, Park C, Kang WK. Statins, 3-hydroxy-3-methylglutaryl coenzyme A reductase inhibitors, potentiate the anti-angiogenic effects of bevacizumab by suppressing angiopoietin2, BiP, and Hsp90alpha in human colorectal cancer. British journal of cancer. 2014; 111: 497-505.

15. Al-Haidari AA, Syk I, Thorlacius H. HMG-CoA reductase regulates CCL17-induced colon cancer cell migration via geranylgeranylation and RhoA activation. Biochemical and biophysical research communications. 2014; 446: 68-72.

16. Lee J, Lee I, Han B, Park JO, Jang J, Park C, et al. Effect of simvastatin on cetuximab resistance in human colorectal cancer with KRAS mutations. Journal of the National Cancer Institute. 2011; 103: 674-88.

17. Fang J, Nakamura H, Maeda H. The EPR effect: Unique features of tumor blood vessels for drug delivery, factors involved, and limitations and augmentation of the effect. Advanced drug delivery reviews. 2011; 63: 136-51.

18. Oft M, Heider KH, Beug H. TGFbeta signaling is necessary for carcinoma cell invasiveness and metastasis. Current biology: CB. 1998; 8: 1243-52.

19. Palmer G, Chobaz V, Talabot-Ayer D, Taylor S, So A, Gabay C, et al. Assessment of the efficacy of different statins in murine collagen-induced arthritis. Arthritis and rheumatism. 2004; 50: 4051-9.

20. Jin R, Zhu X, Liu L, Nanda A, Granger DN, Li G. Simvastatin attenuates stroke-induced splenic atrophy and lung susceptibility to spontaneous bacterial infection in mice. Stroke. 2013; 44: 1135-43.

21. Banciu M, Fens MH, Storm G, Schiffelers RM. Antitumor activity and tumor localization of liposomal glucocorticoids in B16 melanoma-bearing mice. Journal of controlled release: official journal of the Controlled Release Society. 2008; 127: 131-6.

22. Jin W, Gao MQ, Lin ZW, Yang DX. Multiple biomarkers of colorectal tumor in a differential diagnosis model: a quantitative study. World journal of gastroenterology. 2004; 10: 439-42.

23. Jansson A, Sun XF. Bax expression decreases significantly from primary tumor to metastasis in colorectal cancer. Journal of clinical oncology: official journal of the American Society of Clinical Oncology. 2002; 20: 811-6.

24. Gornall AG, Bardawill CJ, David MM. Determination of serum proteins by means of the biuret reaction. The Journal of biological chemistry. 1949; 177: 751-66.

25. Patras L, Sesarman A, Licarete E, Luca L, Alupei MC, Rakosy-Tican E, et al. Dual role of macrophages in the response of C26 colon carcinoma cells to 5-fluorouracil administration. Oncology letters. 2016; 12: 1183-91.

26. Banciu M, Schiffelers RM, Fens MH, Metselaar JM, Storm G. Anti-angiogenic effects of liposomal prednisolone phosphate on B16 melanoma in mice. Journal of controlled release: official journal of the Controlled Release Society. 2006; 113: 1-8.

27. Del Rio D, Stewart AJ, Pellegrini N. A review of recent studies on malondialdehyde as toxic molecule and biological marker of oxidative stress. Nutrition, metabolism, and cardiovascular diseases: NMCD. 2005; 15: 316-28.

28. Ahn KS, Sethi G, Aggarwal BB. Simvastatin potentiates TNF-alpha-induced apoptosis through the down-regulation of NF-kappaB-dependent antiapoptotic gene products: role of IkappaBalpha kinase and TGF-beta-activated kinase-1. Journal of immunology. 2007; 178: 2507-16.

29. De Simone V, Franze E, Ronchetti G, Colantoni A, Fantini MC, Di Fusco D, et al. Th17-type cytokines, IL-6 and TNF-alpha synergistically activate STAT3 and NF-kB to promote colorectal cancer cell growth. Oncogene. 2015; 34: 3493-503.

30. Luput L, Licarete E, Sesarman A, Patras L, Alupei MC, Banciu M. Tumor-associated macrophages favor C26 murine colon carcinoma cell proliferation in an oxidative stress-dependent manner. Oncology reports. 2017; 37: 2472-80.

31. Chen W, Wang J, Jia L, Liu J, Tian Y. Attenuation of the programmed cell death-1 pathway increases the M1 polarization of macrophages induced by zymosan. Cell death & disease. 2016; 7: e2115.